ELSEVIER

Quenching of the excited singlet state of acridine and 10-methylacridinium cation by thio-organic compounds in aqueous solution

Tomasz Pedzinski [a], Bronislaw Marciniak [a,*], Gordon L. Hug [b]

[a] *Faculty of Chemistry, Adam Mickiewicz University, Grunwaldzka St. 6, 60-780 Poznan, Poland*
[b] *Radiation Laboratory, University of Notre Dame, Notre Dame, IN 46556, USA*

Abstract

In this work, the lowest excited singlet states of acridine (Acr), acridinium (AcrH$^+$) and 10-methylacridinium (AcrMe$^+$) are quenched by sulfur-containing amino acids and carboxylic acids in aqueous solution. Both steady-state and time-resolved fluorescence techniques were used to monitor the quenching of fluorescence. Stern–Volmer plots of the fluorescence intensity showed a static component (K_S) to the quenching. The experimental K_S values were compared to theoretical K_S values for outer-sphere complexes based on Debye–Hückel theory and the Fuoss equation. The general agreement between experimental and theoretical K_S values indicate that the static quenching can be attributed to non-fluorescing ion pairs associated as simple outer-sphere complexes. The computed values of the interionic distances of the ion pairs are consistent with the ion pairs of the $Z_A Z_Q = -1$ and -2 cases being solvent-separated ion pairs while those of the $Z_A Z_Q = -3$ case are contact ion pairs. The effect of the reactants' charges on the quenching rate constants (dynamic component) was observed for the reactions of AcrMe$^+$ with the anionic forms of the quenchers (having charges $Z_Q = -1, -2$ and -3). The rate constants (extrapolated to ionic strength, $\mu = 0$) for the quenching processes were determined to be 0.3–$5.3 \times 10^{10}\,\mathrm{M^{-1}\,s^{-1}}$ depending on the ionic charge (Z_Q) of the quencher used. These trends in the quenching rate constants are rationalized with a quenching scheme for electron transfer. Analogous quenching rate constants for alanine and glycine were found to be at least an order of magnitude lower. Photoinduced electron transfer from the sulfur atom of the quencher molecule to the acridine excited singlet state is suggested to be the most likely mechanism of the process under discussion. © 2002 Elsevier Science B.V. All rights reserved.

Keywords: Fluorescence; Quenching; Electron transfer; Acridine; Sulfur-containing amino acids

1. Introduction

A large number of useful chemical and critical biological processes involve electron transfer as a key reaction step that is often accompanied by cleavage or formation of chemical bonds. An important class of such reactions involves sulfur-containing organic compounds (e.g. methionine). Electron transfer is a characteristic reaction of these compounds because of their easily oxidizable thioether groups [1]. The oxidation of sulfur-containing organic molecules has been implicated in biological systems under conditions of oxidative stress [2]. For instance, in Alzheimer's disease, the neurotoxicity of the senile plaques has been associated in part with the oxidation of methionine residues in the

β-amyloid peptides that are major constituents of these plaques [3,4]. Furthermore, oxidation of sulfur-containing, amino acid residues appears to be involved in the pathogenesis of several other diseased states (e.g. cataract formation in eye lenses) [5,6], and their oxidation is of concern because of its possible role in the inactivation of several hormones (e.g. human growth hormone, corticotrophin, parathyroid hormone) [4–6]. Commercially, the oxidation of these compounds has been associated with difficulties in stabilizing pharmaceutically relevant proteins (e.g. interleukin-2 [5] and relaxin [6]).

One approach to gaining an understanding of such complex biological processes is to look at electron transfer in less complicated systems. These model systems can often be further simplified by incorporating photoinitiation. Excited states have two features that make them good model electron-transfer agents. First, they often can initiate clean one-electron-transfer processes, and, second, the very

* Corresponding author. Tel.: +48-61-829-1327; fax: +48-61-865-8008.
E-mail address: bronekm@amu.edu.pl (B. Marciniak).

existence of excited species can be externally controlled by the investigator.

Photo-oxidation of sulfur-containing compounds, i.e. aliphatic thioethers [7], carboxylic acids [8], amino acids [9–11], has been the subject of several steady-state and flash photolysis studies where photosensitization was through aromatic ketones. The primary photochemical step in these reactions involves an electron transfer from the sulfur atom to the excited triplet state of the aromatic ketone. The electron-transfer nature of the process was suggested by the large values of the quenching rate constants (k_q in the range $10^9 \, M^{-1} \, s^{-1}$) and by the direct observation of radical species—the products of electron-transfer reactions, e.g. the ketyl radical anion of benzophenone and sulfur-centered radical cations $(S \therefore S)^+$.

Excited states of aromatic aminium cations are potentially good electron acceptors to sensitize the oxidation of thioethers. In *N*-(9-methylpurin-6-yl)pyridinium cation, both singlet (335 kJ/mol) and triplet states (268 kJ/mol) proved to be efficient photosensitizers for one-electron-transfer reactions with thioethers [12]. Its E_{red} is $-0.57 \, V$ vs. SCE in its ground state [13]. Acridinium cations have lower photo-excitation energies than this pyridinium cation. For instance, 10-methylacridinium has a photo-excitation energy roughly equal to the energy of the triplet state of *N*-(9-methylpurin-6-yl)pyridinium, and its ground state has $E_{red} = -0.46 \, V$ vs. SCE [14], making it potentially almost as good an electron acceptor as the triplet state of *N*-(9-methylpurin-6-yl)pyridinium. However, it has the advantage of having a lower photo-excitation energy, and thereby is a more flexible probe. In this work, the nature of the quenching by thioethers of these popular acridine fluorescence probes is explored.

2. Experimental

2.1. Materials

-

Methylacridinium iodide was prepared by the reaction of acridine with methyl iodide in acetonitrile, and it was converted to the perchlorate salt $(AcrMe^+ ClO_4^-)$ by the addition of magnesium perchlorate to the iodide salt. It was purified by recrystallization from ethanol. Acridine (Acr) was obtained commercially from Sigma. The sulfur-containing amino and carboxylic acids (Table 1) were also obtained commercially from Sigma (**1, 2, 4–11**), Aldrich (**12, 13**) and Reanal-Hungary (**3**) as the best purity grades available. These compounds were used without further purification. Water was purified with a Millipore Milli-Q system.

2.2. Solutions

In the quenching experiments, the concentrations of the acridine derivatives were varied between 1×10^{-5} and $5 \times$

Table 1
Ground-state pK_a values of sulfur-containing amino and carboxylic acids [19]

Number	Quencher	pK_a
1	Methionine	2.10, 9.06
2	Ethionine	2.18, 9.05
3	Cysteine	1.71, 8.36
4	Thiaproline	1.5, 6.11
5	α-Methylmethionine	2.2, 9.10
6	*S*-Carboxymethylcysteine	1.99, 3.36, 8.89
7	*S*-Carboxyethylcysteine	2.14, 4.36, 9.08
8	3,3′-Thiodipropionic acid	3.90, 4.67
9	2,2′-Thiodiethanoic acid	3.15, 4.13
10	3-(Carboxymethylthio)propionic acid	3.27, 4.34
11	2-(Carboxymethylthio)succinic acid	3.26, 3.79, 5.12
12	Alanine	2.35, 9.87
13	Glycine	2.35, 9.78

$10^{-5} \, M$. Fresh solutions were made just before each experiment and were not deoxygenated in the fluorescence experiments. The concentrations of the quenchers were in the range $(0.5–5) \times 10^{-2} \, M$. In the flash photolysis studies, solutions were deoxygenated, and the concentration of 10-methylacridine was $1 \times 10^{-5} \, M$ while that of the quencher varied up to 0.5 M. The pH of the solutions was adjusted by adding NaOH or HCl. $NaClO_4$ was used to set the desired ionic strength of the solution.

2.3. Methods

Absorption spectra were recorded with a Hewlett-Packard 8452A diode array spectrophotometer, and the steady-state fluorescence spectra were recorded using a Perkin-Elmer LS 50 B spectrofluorometer. Fluorescence lifetime measurements were carried out using the time-correlated single-photon counting technique. Both a nanosecond system from IBH Consultants, Model 5000, and a picosecond system were used. The picosecond system [15] (those experiments were carried out in the Centre for Ultrafast Laser Spectroscopy located at Adam Mickiewicz University, Poznan, Poland) was equipped with the Ti:Sapphire "Tsunami" laser, pumped with an argon ion laser Beam Lock 2060, tunable in the 720–1000 nm region, generating 1–2 ps pulses at a repetition rate of about 82 MHz, and having a mean power of over 1 W. A harmonic generator, model GWU-23PS, was used for doubling and tripling the exciting-beam frequency. The pulse-timing and data-processing subsystems employed a biased time-to-amplitude converter (TAC), model TC 864 (Tennelec). The emission was detected with a microchannel plate (MCP), model R3809U-05. The MCP was thermo-electrically cooled, and its output signal was amplified (Hamamatsu). The standard procedure for performing these measurements included taking an instrument profile and counting photon signals until at least 10^4 counts were collected at the maxima of the fluorescence decay histograms.

The laser flash photolysis experiments were carried out using the new detection system in the Radiation Laboratory
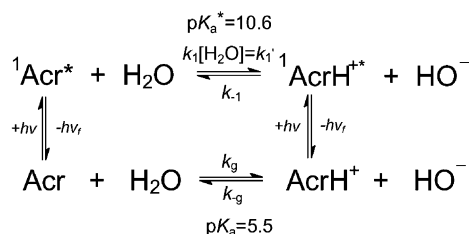
at the University of Notre Dame [16]. The laser used in these experiments was a nitrogen laser from Laser Photonics PRA/Model UV-24 for excitation at 337.1 nm. The energy deposited was controlled to be approximately 6 mJ/pulse, and the pulse length was approximately 8 ns (full width at half height). In the nanosecond laser flash photolysis experiments, oxygen was removed from the solutions by bubbling them with high-purity argon for at least 15 min.

The van der Waals radii of $AcrMe^+$ and the quenchers were computed using HyperChem 5.1 Pro from Hypercube.

3. Results and discussion

When an acridine molecule is excited to its S_1 state (Acr^*), the excited species becomes a much stronger proton acceptor than the ground state. The pK_a of protonated acridine increases from $pK_a = 5.5$ in its ground state to $pK_a^* = 10.6$ [17] in its lowest excited singlet state. These processes are depicted in Scheme 1, which illustrates the acid–base equilibria of acridine and its singlet excited state in water. In aqueous solution at room temperature with the pH between the pK_a of the ground state and the pK_a^* ($pK_a < pH < pK_a^*$), excited acridine undergoes protonation and forms the excited acridinium cation ($AcrH^{+*}$). As a consequence, under these conditions, fluorescence can be observed from both, neutral ($\lambda_{max} = 425$ nm) and cationic forms ($\lambda_{max} = 475$ nm). On the other hand, at pH above the pK_a^* only fluorescence from the unprotonated species (Acr^*) is observed, and, at pH below the pK_a of the ground state, only the fluorescence from acridinium cation ($AcrH^{+*}$) can be observed. Thus, the pH of the solution can be used to control the nature of the excited state, and most of the experiments with excited acridinium cations were carried out at pH 3.5–4.0, whereas experiments on excited neutral acridine were performed at pH ≥ 11.0. In the former pH region, the excited state and the ground state are both protonated, whereas, in the latter pH region, both states are unprotonated. The fluorescence decay traces and fluorescence spectral shapes indicate the existence of only the expected forms of excited acridine under the conditions mentioned above.

Such complex acid–base behavior is not observed for the 10-methylacridinium cation ($AcrMe^+$). However, most experiments with $AcrMe^+$ were done at slightly acidic pH in order to avoid the ground-state reaction of $AcrMe^+$ with OH^- [18].

$$pK_a^* = 10.6$$
$${}^1Acr^* + H_2O \underset{k_{-1}}{\overset{k_1[H_2O]=k_{1'}}{\rightleftharpoons}} {}^1AcrH^{+*} + HO^-$$
$$+h\nu \Big\updownarrow -h\nu_f \qquad\qquad +h\nu \Big\updownarrow -h\nu_f$$
$$Acr + H_2O \underset{k_{-g}}{\overset{k_g}{\rightleftharpoons}} AcrH^+ + HO^-$$
$$pK_a = 5.5$$

Scheme 1.

The quenching of *N*-(9-methylpurin-6-yl)pyridinium cation fluorescence by sulfur-containing amino and carboxylic acids was found to occur via electron transfer [12]. Since the related aminium cations, the acridines, have significantly less negative, but still substantial, free-energy changes (ΔG_{el}) for the transfer of an electron to their excited singlet states from thioethers (see below), it is of interest to see if electron transfer can occur efficiently with these photosensitizers. Motivated by this, we have investigated the interaction of different acridine derivatives with thio-organic compounds in aqueous solution. The fluorescence quenching rate constants k_q of Acr, $AcrH^+$ and $AcrMe^+$ were measured for a selected series of quenchers. The series included some relatively easily oxidizable sulfur-containing amino and carboxylic acids (Table 1). For comparison, two non-sulfur-containing amino acids were included in the series of quenchers under investigation. The pH of the aqueous solutions was controlled so that the ionic nature of the sensitizers and the quenchers was easy to identify (see below).

For the quenching experiments, the appropriate pH of the solution was set in order to study the interaction between a specific ionic form of the acridine and specific ionic forms of the quencher. Amino acids **1–5** and **12–13** were in their zwitterionic forms, while quenchers **6**, **7**, **8–10** and **11** carried net electric charges of -1, -2 and -3, respectively. However, one should notice that some of the quenchers studied (compounds **4–11**) can exist in the experimental solution in different anionic forms, as well as being in the zwitterionic form. The presence of the various species depends on the pK_a value of the quencher and the pH of the solution (vide Table 1).

It is well known [20] that cationic dyes such as $AcrMe^+$ and $AcrH^+$ act as electron acceptors and can possibly form ground-state charge-transfer complexes with electron donors:

$$AcrMe^+ + Q^{-Z_Q} \rightleftharpoons (AcrMe^+ \cdots Q^{-Z_Q}) \qquad (1)$$
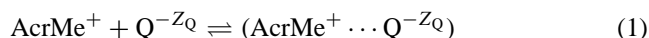
Therefore, the fluorescence quenching of these acridine derivatives by sulfur-containing organic species could have a static contribution in addition to dynamic quenching processes. Absorption spectra of all the acridines studied are shown in Fig. 1. UV–visible absorption measurements did not show any extraneous absorptions that could be attributed to ground-state complexation even at higher quencher concentrations (up to 0.1 M). The only evidence for ground-state complex formation came from measurements of fluorescence intensity (I_f^0 in the absence and I_f in the presence of quenchers). Specifically, Stern–Volmer plots (I_f^0/I_f vs. [Q]) of steady-state fluorescence quenching for all the acridines show a distinct, upward curvature (Fig. 2). This curvature is seen mainly for higher concentrations of the quenchers. In contrast, the plots from fluorescence lifetime measurements (τ^0/τ vs. [Q]) are perfectly linear over the whole range of the quencher concentrations used. τ^0 is the lifetime of the excited singlet state of an acridine in the absence of a quencher and τ the lifetime of the excited singlet state of
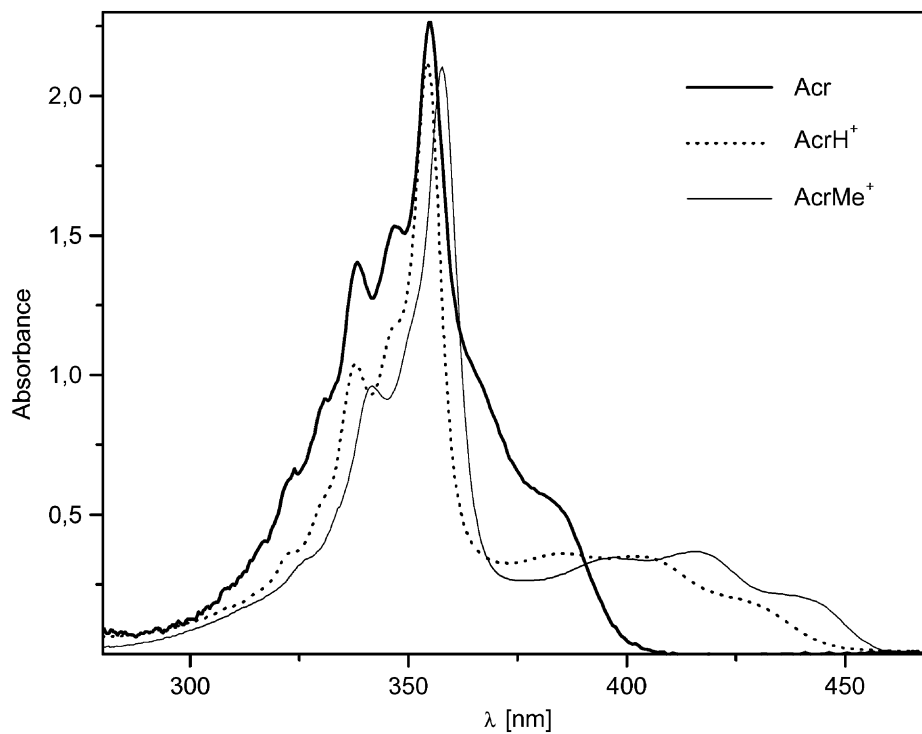
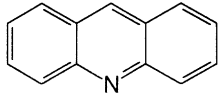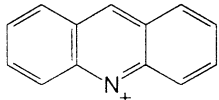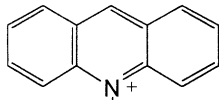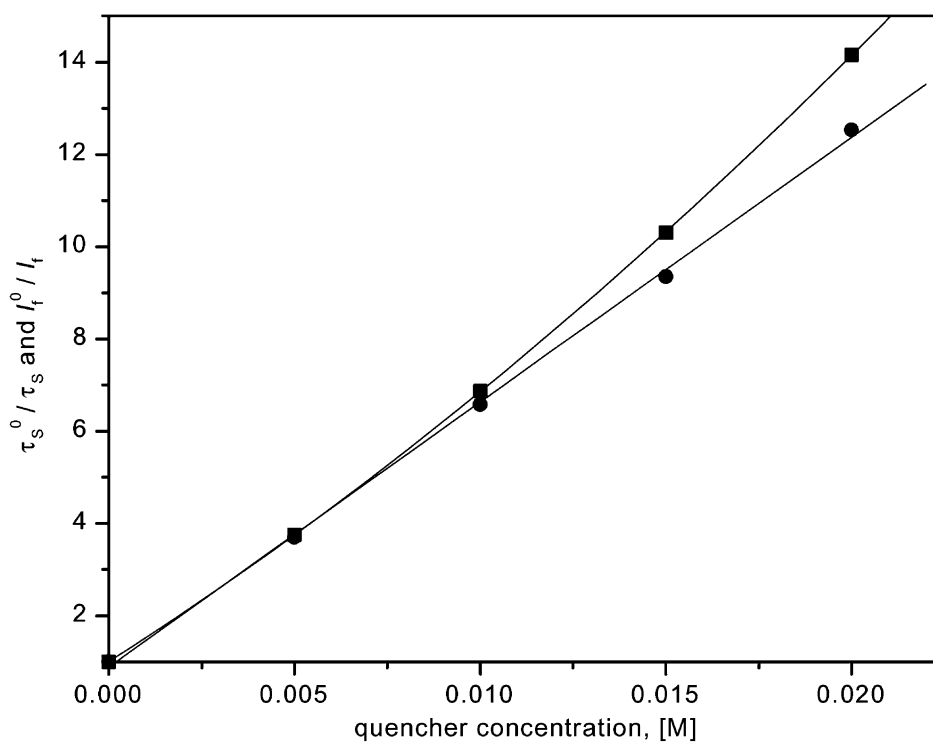Fig. 1. The set of acridine derivatives' absorption spectra in water.

Fig. 2. Stern–Volmer plots for quenching of $^1(\mathrm{AcrMe}^+)^*$ by 3,3′-thiodipropionic acid ($Z_A Z_Q = -2$ at pH 6.0) based on fluorescence lifetimes (circles) and fluorescence intensity (squares) measurements (at constant ionic strength $\mu = 0.12\,\mathrm{M}$).

Table 2
Rate constants for quenching of acridine and its derivatives' fluorescence in aqueous solution

	Quencher	$Z_A Z_Q$	$k_q \times 10^{-9}$ $(M^{-1} s^{-1})$[a]	$k_q^{\mu=0} \times 10^{-9}$ $(M^{-1} s^{-1})$
Acr	Methionine	0	3.45 ± 0.10	–
	Thiaproline	0	3.91 ± 0.10	–
	Ethionine	0	3.50 ± 0.15	–
	Cysteine	0	3.60 ± 0.10	–
	α-Methylmethionine	0	4.10 ± 0.20	–
	S-Carboxymethylcysteine	0	4.37 ± 0.20	–
	S-Carboxyethylcysteine	0	4.10 ± 0.20	–
	3,3'-Thiodipropionic acid	0	3.90 ± 0.15	–
	2-(Carboxymethylthio)succinic acid	0	4.7 ± 0.20	–
	Glycine	0	0.044 ± 0.005	–
	Alanine	0	0.02 ± 0.01	–
AcrH$^+$	Methionine	0	3.4 ± 0.1	–
	Thiaproline	0	3.2 ± 0.1	–
	Ethionine	0	3.95 ± 0.15	–
	α-Methylmethionine	0	4.1 ± 0.20	–
	Glycine	0	0.044 ± 0.01	–
	Alanine	0	0.019 ± 0.004	–
AcrMe$^+$	Methionine	0	4.1 ± 0.2	–
	α-Methylmethionine	0	3.9 ± 0.2	–
	S-Carboxymethylcysteine	−1	13.4 ± 1.0[b]	20.4 ± 1.9
	S-Carboxyethylcysteine	−1	14.1 ± 0.6[b]	23.1 ± 2.4
	3,3'-Thiodipropionic acid	−2	17.0 ± 0.3[b]	37.8 ± 2.0
	2,2'-Thiodiethanoic acid	−2	17.9 ± 0.7[b]	34.3 ± 2.4
	3-(Carboxymethylthio)propionic acid	−2	17.6 ± 1.0[b]	32.9 ± 2.1
	2-(Carboxymethylthio)succinic acid	−3	22.1 ± 1.5[b]	52.7 ± 3.9

[a] Errors were computed as twice the standard deviation from the least-squares fit method.
[b] At constant ionic strength $\mu = 0.04$ M.

an acridine in the presence of a quencher. Single exponential decays were observed for all quenchers and solutions measured. The fluorescence quenching rate constants, k_q, were determined from the slopes of the τ^0/τ vs. [Q] plots, and the resulting k_q values are reported in Table 2.

We believe that the most likely explanation of the behavior described above is a result of the formation of a non-fluorescent complex (ion pair association in the ground state). When there is such a static quenching process in addition to a dynamic quenching component, the steady-state fluorescence intensity can be analyzed using the following equation [21]:

$$\frac{I_f^0}{I_f} = (1 + K_D[Q])(1 + K_S[Q]) \qquad (2)$$

where $K_D = \tau^0 k_q$ and $K_S = [A\cdots Q]/([A][Q])$. In the expression for K_S, [A] is the concentration of the non-complexed, ground-state acridine derivative in the presence of quencher. A comparison of the constants K_S and K_D is summarized in Table 3 and indicates that the contribution from the dynamic term is the main quenching process. Since K_S is quite small compared to K_D, an alternate computation procedure was used to check the validity of the result. From the lifetime measurements $K_D' = k_q \tau^0$ was computed, and K_S' was computed from K_D' and Eq. (2). A comparison of the respective values of K_D vs. K_D' and K_S vs. K_S' in Table 3 shows that there can be a meaningful determination of the static and dynamic components in the quenching process.

Table 3
Contribution of the static and dynamic terms in the quenching of AcrMe$^+$ fluorescence measured at pH 6.0 and at constant ionic strength $\mu = 0.12$ M

Quencher	$Z_A Z_Q$	K_D (M^{-1})[a]	K_S (M^{-1})[a]	K_D' (M^{-1})[b]	K_S' (M^{-1})[b]
1	0	138 ± 7[c]	Not observed	138 ± 7[c]	Not observed
6	−1	385 ± 23	6.6 ± 3	385 ± 10	6.5 ± 2.6
8	−2	363 ± 22	12.5 ± 2	383 ± 8	11.7 ± 2.1
11	−3	362 ± 15	16.5 ± 2	396 ± 11	15.0 ± 2.9

[a] Both K_D and K_S values were computed from polynomial fit (second-order) based on fluorescence intensity measurements.
[b] K_D' values were computed from the experimentally obtained k_q and $\tau = 33.7$ ns; K_S' values were computed from Eq. (2) and the respective K_D' values.
[c] Value computed from linear fit.

For solutions with $Z_A Z_Q \neq 0$, the quenching parameter K_S is physically an association constant between ion pairs and free ions. The Fuoss expression [22]

$$K_S = \frac{4\pi N a^3}{3000} \exp\left(-\frac{Z_A Z_Q e^2}{\varepsilon a k_B T}\right) \tag{3}$$

and related variants of it have been used successfully to compute the equilibrium constant (in M^{-1}) between ion pairs and free ions for describing outer-sphere association constants [23]. In Eq. (3), a (in cm) is the ion-pair's interionic distance and ε the dielectric constant. This form of the Fuoss equation is based on the Debye–Hückel screened Coulomb, interionic potential energy

$$U(a) = \frac{Z_A Z_Q e^2}{\varepsilon a} - \frac{Z_A Z_Q e^2 \kappa}{\varepsilon(1 + \kappa a)} \tag{4}$$

where $1/\kappa$ is the Debye screening length

$$\kappa^2 = \frac{8\pi N e^2 \mu}{1000 \varepsilon k_B T} \tag{5}$$

at the ionic strength μ (in M). This form of the theory allows for the finite size of the ions [24]. The screening is incorporated implicitly in the expression for K_S, in which the Debye–Hückel expression for activity coefficient was used [22].

The interionic distance of the various ion pairs can be computed from the experimental K_S values in Table 3 and Eq. (3), under the assumption that the ion pairs are simple outer-sphere complexes (spherical reactants in contact) [22]. The final equation for the unknown interionic distance, a, is a transcendental equation (in a^3 and $\exp\{1/a\}$) and was solved by a graphical method. The values of a were 11.2 Å (9.6–14.4 Å), 10.8 Å (10.0–11.7 Å) and 7.2 Å (only near-crossing in graphical solution) for $Z_A Z_Q = -1, -2$ and -3, respectively. (The intervals in parentheses are the limits of the standard deviation ranges of K_S, Table 3.) The center-to-center distances between the ions for $Z_A Z_Q = -1$ and -2 are slightly larger than the sum of the van der Waals radii computed from the geometry of the molecule including a solvent shell of 1.4 Å. Without the solvent shell, the sum of the radii was computed to be approximately 8 Å.

The general trend of smaller interionic distances with increased charge on the quencher anions is an indication that the high electric field may be perturbing the medium. Above an electric field of 1×10^4 V/cm, Böttcher [25] states that dielectric saturation can play a role. At $a = 10.8$ Å for $Z_A Z_Q = -2$, the electric field due to the anion at the center of the ground-state acridine is 3.6×10^5 V/cm. For $Z_A Z_Q = -3$ and $a = 7.2$ Å, the electric field due to the anion at the center of the excited acridine is 1×10^6 V/cm. The change in the dielectric constant at high fields due to dielectric saturation can be written as [25]

$$\Delta \varepsilon = -\frac{4\pi N \mu_d^4}{45(k_B T)^3} \frac{\varepsilon_0^4 (\varepsilon_\infty + 2)^4}{(2\varepsilon_0 + \varepsilon_\infty)^2 (2\varepsilon_0^2 + \varepsilon_\infty^2)} E^2 \tag{6}$$

where ε_0 is the dielectric constant at low field (80 for water), ε_∞ the high frequency dielectric constant ($n^2 = 1.78$ for water), μ_d the permanent dipole moment of the solvent molecules (1.85 debye for water), and E the electric field amplitude at the point under consideration. Substituting these values into Eq. (6) gives $\Delta \varepsilon = -1$ for $Z_A Z_Q = -2$ and $\Delta \varepsilon = -8.7$ for $Z_A Z_Q = -3$. Since the latter number could have a significant effect, the graphical solution for a was repeated with $\varepsilon = 71$. The graphical solution still does not formally exist for this dielectric constant, but the distance, at which the curves come very close, shifts to approximately 7.5 Å, slightly larger than for $\varepsilon = 80$. Thus although dielectric saturation is significant at the high electric field in the ion pair for $Z_A Z_Q = -3$, the interionic distance, itself, does not change significantly.

The interionic distance for $Z_A Z_Q = -3$ is in the lower part of the computed (by HyperChem) range of van der Waals radii for these ion pairs. In addition, this distance does not change significantly even when the dielectric saturation is taken into account. On the other hand, the interionic distance for $Z_A Z_Q = -1$ and -2 are at the upper end of the computed (by HyperChem) range of van der Waals radii that correspond to the ions each being surrounded by solvent shells. Even accounting for the experimental error bars quoted above, the two cases for $Z_A Z_Q = -1$ and -2 are distinctly separate from the $Z_A Z_Q = -3$ case. The values for these three cases are consistent with the ion pairs of the $Z_A Z_Q = -1$ and -2 cases being solvent-separated ion pairs while those of the $Z_A Z_Q = -3$ case are contact ion pairs.

Since the results obtained from steady-state fluorescence quenching experiments are complicated by the static component, we concentrate in the rest of the discussion on the analysis of the time-resolved results (dynamic quenching) (see Fig. 3 for a typical example). The rate constants k_q for the fluorescence quenching of all acridine derivatives by sulfur-containing amino and carboxylic acids in their zwitterionic form (compounds **1**–**5**) are in the range $(3.2–4.1) \times 10^9$ M^{-1} s^{-1} (see Table 2). These values for the quenching rate constants are approaching nearly half of the diffusion-controlled limit [26]. Moreover, the rate constants for the quenching of Acr (neutral acridine) by all the sulfur-containing quenchers (including those carrying negative charge) also reach approximately one-half of the diffusion-controlled limit, $k_q = (3.5–4.7) \times 10^9$ M^{-1} s^{-1}. On the other hand, for non-sulfur-containing compounds (i.e. alanine and glycine), the k_q values are at least one order of magnitude lower than those observed for the analogous compounds, containing a sulfur moiety. Similar differences were seen in the efficiency of the fluorescence quenching of N-(9-methylpurin-6-yl)pyridinium cations by the quenchers mentioned above [12]. This may suggest that, like the case for this pyridinium cation, the quenching of all the acridines investigated involves an electron transfer from the sulfur atom as the primary step in the quenching process that we have been describing.
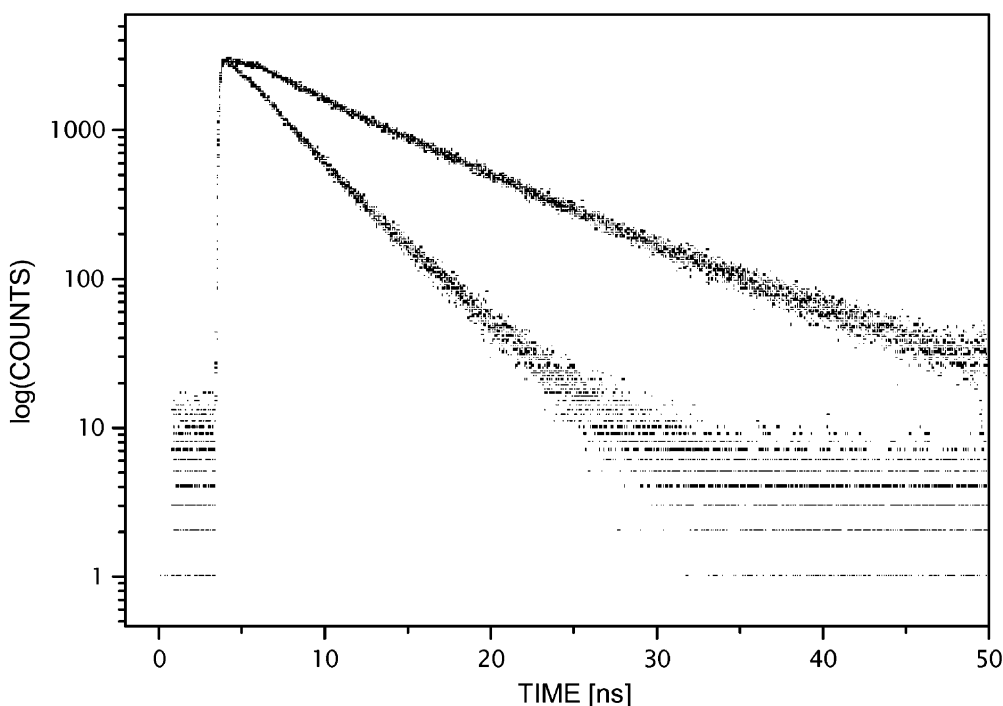
Fig. 3. Time-resolved measurements of Acr fluorescence (unquenched and quenched by methionine, [Met] = 0.02 M) monitored at 425 nm in water at pH 7.5.

The involvement of electron transfer as the mechanism of the quenching process can also be supported by the large value of $\Delta G_{el} \approx -120$ kJ/mol (for AcrMe$^+$) from the Weller equation [27]:

$$\Delta G_{el} = F(E_{ox} - E_{red}) - E_S + \Delta w \qquad (7)$$

where E_{ox} is the reduction potential of the oxidized radical going to the quencher and E_{red} the reduction potential of the ground state of the acridine. To calculate a representative value, we took E_{ox} for methionine as 1.1 V vs. SCE [28], the reduction potential for AcrMe$^+$ as $E_{red} = -0.46$ V vs. SCE [14], $E_S = 268$ kJ/mol [29] and $\Delta w = 0$ [12]. The analogous free-energy changes are similar for the quenching of the lowest excited singlet states of AcrH$^+$ and Acr.

Since AcrMe$^+$ exists in its ionic form, the quenching rate constant should depend on the ionic strength (μ) for compounds **6–9** (quenchers carrying negative charge) [30]. This expectation is based on the Debye–Hückel theory for the electrolytes' screening of the Coulomb potential between the charged excited species and the charged quenchers. Our analysis was done using the modified form of the Debye–Hückel kinetic equation [30]

$$\log\left(\frac{k_q}{k_q^{\mu=0}}\right) = 1.02 Z_A Z_Q \frac{\sqrt{\mu}}{1 + \sqrt{\mu}} \qquad (8)$$

This version of the primary salt effect is derived from the form of the interionic potential energy, Eq. (4), that allows for the finite sizes of the ions [30]. Therefore, we examined the influence of the ionic strength on the quenching rate constant in all of these systems, using NaClO$_4$ to control the value of μ. The results are presented in Fig. 4 and show the expected [26,30] functional dependence for the various charges ($Z_A = +1$ and $Z_Q = -1, -2$ or -3). In particular, the slopes of the plots of $\log(k_q/k_q^{\mu=0})$ vs. $\sqrt{\mu}/\sqrt{\mu}+1$ give approximately the expected slopes of $1.02 Z_A Z_Q$.

By using Eq. (8) to extrapolate to zero ionic strength, the effects of ionic screening on the quenching rate constants can be eliminated for the purpose of making comparisons between systems having different charges on the reactants. For uncharged Acr, the rate constant for its singlet quenching was found to be independent of the value of the ionic strength. The same independence was found for quenching the other acridine sensitizers (i.e. AcrH$^+$ and AcrMe$^+$) by the zwitterionic forms of the amino acids. This behavior is consistent with $Z_A Z_Q = 0$ in Eq. (8).

The quenching rate constants, determined for constant ionic strength and those extrapolated to $\mu = 0$, are summarized in Table 2. Not unexpectedly [31], and as described above, any of the reactions that involve a species carrying no charge (e.g. amino acids in their zwitterionic forms) have k_q values for quenching that are lower than the $k_q^{\mu=0}$ values for the reactions of cations (i.e. AcrMe$^+$) with anionic quenchers. In the latter type of reaction between excited singlets of AcrMe$^+$ and anions of varying charge, the extrapolated quenching rate constants increase with increasing negative charge on the quencher, Q. In summary, $k_q(Q^0) < k_q^{\mu=0}(Q^{-1}) < k_q^{\mu=0}(Q^{-2}) < k_q^{\mu=0}(Q^{-3})$.
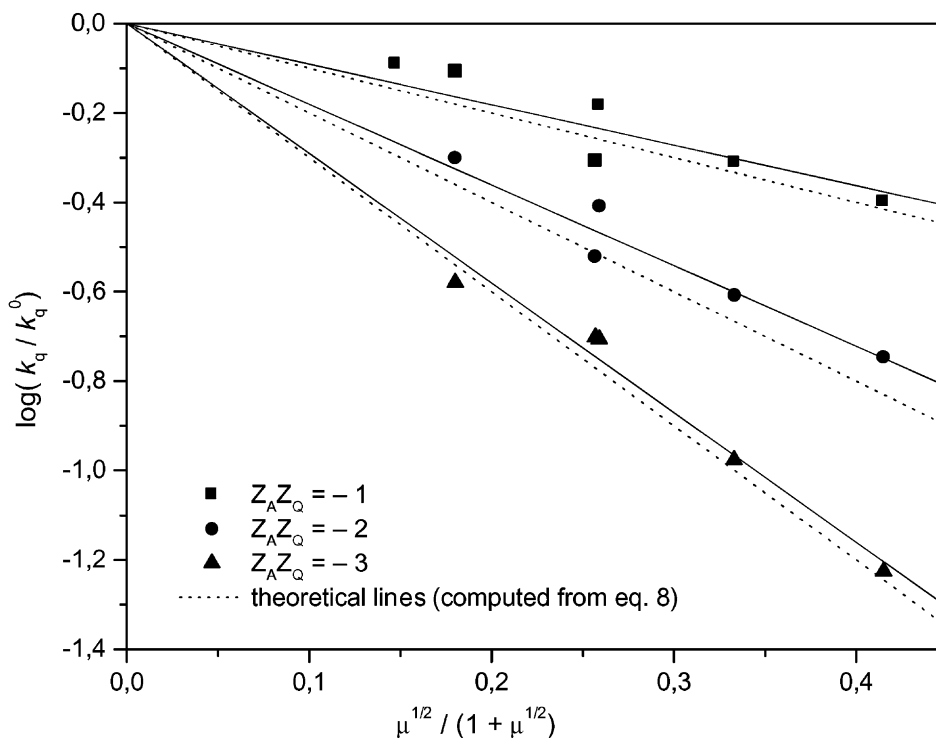
Fig. 4. Variation of the quenching rate constants k_q with ionic strength of the aqueous solution for quenching of AcrMe$^+$ fluorescence by **6** ($Z_A Z_Q = -1$), **8** ($Z_A Z_Q = -2$) and **11** ($Z_A Z_Q = -3$).

The effect of the reactants' charges on the quenching rate constants can be explained by the change in diffusion-controlled rate constants, k_d and k_{-d}, as a function of the product of reactants' charges $Z_A Z_Q$ (see Ref. [12]) using Scheme 2 for electron-transfer quenching. The highly negative value of ΔG_{el} allows (see above) us to make an assumption that the overall quenching rate constants have reached a plateau value similar to the ones observed and analyzed for triplet quenching by thioethers [28]. The expression for the plateau value is [28]

$$k_q^{max} = \frac{k_{el}^0 k_d}{k_{el}^0 + k_{-d}} \qquad (9)$$

where k_{el}^0 is the pre-exponential factor in the relation for the forward electron-transfer rate constant

$$k_{el} = k_{el}^0 \exp\left(\frac{-\Delta G_{el}^{\neq}}{RT}\right) \qquad (10)$$

The expression for k_q^{max} in Eq. (9) is the limiting ($k_{el} \gg k_{-el}$) value of the quenching rate constant (see above for a justification of this assumption) after making the steady-state approximation for various intermediates in Scheme 2 [28]. In Eq. (9), k_d can be written as [30]
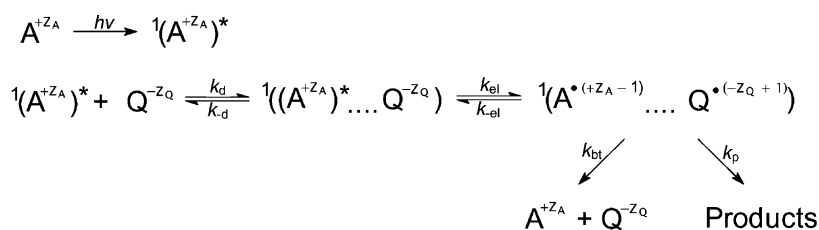
$$k_d = \frac{4\pi(D_A + D_Q)N}{1000} \frac{-Z_A Z_Q r_0}{1 - \exp(Z_A Z_Q r_0/R)} \qquad (11)$$

and k_{-d} can be written from the Eigen equation [32] as

$$k_{-d} = \frac{3(D_A + D_Q)}{R^3} \frac{Z_A Z_Q r_0}{1 - \exp(-Z_A Z_Q r_0/R)} \qquad (12)$$

where D_A and D_Q are the diffusion constants of the acridines and quenchers, respectively, R the reaction distance and the Onsager radius, r_0, is defined by

$$r_0 = \frac{e^2}{\varepsilon k_B T} \qquad (13)$$

$$A^{+Z_A} \xrightarrow{h\nu} {}^1(A^{+Z_A})^*$$

$$^1(A^{+Z_A})^* + Q^{-Z_Q} \underset{k_{-d}}{\overset{k_d}{\rightleftharpoons}} {}^1((A^{+Z_A})^* \dots Q^{-Z_Q}) \underset{k_{-el}}{\overset{k_{el}}{\rightleftharpoons}} {}^1(A^{\bullet(+Z_A-1)} \dots Q^{\bullet(-Z_Q+1)})$$

$$\swarrow k_{bt} \qquad \searrow k_p$$

$$A^{+Z_A} + Q^{-Z_Q} \qquad \text{Products}$$

A$^{+Z_A}$ refers to Acr, AcrH$^+$ and AcrMe$^+$

Scheme 2.

The rate constants, $k_q^{\mu=0}$, extrapolated to zero ionic strength can be compared to the diffusion-controlled rate constants, k_d, computed from Eq. (11) if reaction distances can be estimated. As a rough estimate, the interionic radii, a, determined from K_S in Eq. (3) were used to compute the various k_d values from Eq. (11) for the cases of $Z_A Z_Q = -1$, -2 and -3. The resulting diffusion-controlled rate constants are 2.4×10^{10}, 2.9×10^{10} and $3.4 \times 10^{10}\,M^{-1}\,s^{-1}$, respectively. The extrapolated $k_q^{\mu=0}$ values for $Z_A Z_Q = -1$ and -2 in Table 2 are within experimental error of their respective k_d values, with the $k_q^{\mu=0}$ values for $Z_A Z_Q = -1$ being slightly below their k_d and the $k_q^{\mu=0}$ values for $Z_A Z_Q = -2$ being slightly higher than their k_d.

The $k_q^{\mu=0}$ for the single quenching pair for $Z_A Z_Q = -3$ is distinctly above the computed k_d value. Arriving at such an unrealistic rate constant might be attributed to the extrapolation procedure for obtaining $k_q^{\mu=0}$ where some of ionic strengths were higher than normally used in Debye–Hückel applications. However, since the lower ionic strengths were in the usual range for validity of the theory and since the slopes of the extrapolation were consistent with the theory, there are reasons to accept the extrapolated $k_q^{\mu=0}$ as valid. Possible reasons why $k_q^{\mu=0} > k_d$ for $Z_A Z_Q = -3$ are that $(D_A + D_Q)$ may be different than the value of $2 \times 10^{-5}\,cm^2/s$ assumed in the calculation of k_d or that R may be larger than $7.5\,Å$ obtained from K_S (accounting for dielectric saturation).

The immediately preceding discussion can be taken to support the conclusion that the $k_q^{\mu=0}$ values for $Z_A Z_Q = -1$, -2 and -3 are all essentially diffusion controlled. On the other hand, the values for $Z_A Z_Q = 0$ are roughly half the diffusion-controlled limit. Even though there is an electrostatic work term [30] in the activated step that depends on $Z_A Z_Q$, the electron-transfer rate constant should not depend strongly on the electrostatic work term in water. To first approximation, consider k_{el}^0 in Eq. (9) for k_q^{max} to be approximately constant for the types of sulfur-containing quenchers in Table 2. (This assumption will be consistently held throughout the following computations.) However, even if k_{el}^0 is assumed to be constant for all $Z_A Z_Q$, the denominators in Eq. (9) will vary with $Z_A Z_Q$ because k_{-d} is dependent on $Z_A Z_Q$ as in Eq. (12). As long as k_{el}^0 is much greater than k_{-d}, the denominator in Eq. (9) is approximately equal to k_{el}^0, and then k_{el}^0 cancels out, leaving $k_q^{max} \approx k_d$. This is what appears to be happening for the cases of $Z_A Z_Q = -1$, -2 and -3.

Furthermore, this is consistent with computations from k_{-d} in Eq. (12). For $Z_A Z_Q = 0$, k_{-d} can be derived from Eq. (12) by l'Hospital's rule as $k_{-d} = 3(D_A + D_Q)/R^2$. Taking $R = 7\,Å$ and $D_A + D_Q = 2 \times 10^{-5}\,cm^2/s$, as before, $k_{-d} = 1.2 \times 10^{10}\,s^{-1}$. If k_q^{max} for $Z_A Z_Q = 0$ is approximately half of diffusion controlled, as observed above, then k_{el}^0 by Eq. (9) is also approximately $10^{10}\,s^{-1}$.

To complete the picture, k_{-d} can be computed for the other three cases to be 3.4×10^9, 2.5×10^9 and $1.9 \times 10^9\,s^{-1}$ for $Z_A Z_Q = -1$, -2 and -3, respectively. These latter three rates are distinctly less than the $k_{el}^0 \approx 10^{10}\,s^{-1}$, estimated above. With such a high value of k_{el}^0 compared to the k_{-d} values for $Z_A Z_Q = -1$, -2 and -3, $k_q^{max} \approx k_d$ by Eq. (9). These estimations along with Scheme 2 show how the extrapolated rate constants for $Z_A Z_Q = -1$, -2 and -3 can plausibly be diffusion controlled while the quenching rate constants for $Z_A Z_Q = 0$ only approach half diffusion controlled. This analysis shows how Scheme 2, along with the assumption that k_{el}^0 did not change with $Z_A Z_Q$, leads to a semi-quantitative rationalization of the observed trends in the quenching rate constants for all cases involving sulfur compounds.

Additional insight into the nature of the quenching process could be gained by checking for optically observed transients using nanosecond laser flash photolysis. In order to minimize the possibility of interference from triplet states, the 10-methylacridinium cation was chosen for these experiments because the intersystem crossing quantum yield, $\Phi_{isc} < 0.001$. This estimate was based on relative actinometry [33] with the triplet of 4-carboxybenzophenone in water as the reference, $\varepsilon_{535} = 6250\,M^{-1}\,cm^{-1}$ [34]. Possible transients from electron-transfer quenching would be the acridinyl radical, $\lambda_{max} \approx 500\,nm$ [35], and the intermolecularly (S∴S)-bonded radical cation, with a broad band around $\lambda_{max} = 480\,nm$ [36]. Neither transient was observed on laser excitation of AcrMe$^+$ in the presence of methionine, thiaproline and 3-(methylthio)propanol. This sulfur-containing alcohol was used because of its known, relatively high Φ_{SS^+} [37–39] (SS$^+$ refers to the $\sigma\sigma^*$ 3-electron-bonded radical cation formed upon association of an oxidized sulfide with an unoxidized second sulfide molecule), as well as its high solubility in water. This observation is still consistent with electron-transfer quenching if back-electron transfer is the dominant path for the course of the ensuing reactions. Fast back-electron transfer in the singlet radical pair, initially formed in the quenching complex, is also consistent with the spin-allowed nature of this reverse process. This is in contrast to the spin-forbidden back-electron transfer in the quenching of triplet N-(9-methylpurin-6-yl)pyridinium where electron-transfer products were observed as transients in laser flash photolysis [13].

Scheme 2 illustrates the quenching of the singlet state of acridine (and its derivatives) by thio-organic compounds in aqueous solution. In the scheme, k_{-d} is the rate constant of the dissociation of the encounter complex $^1((A^{+Z_A})^* \cdots Q^{-Z_Q})$, k_{el} and k_{-el} are the rate constants for electron transfer, k_{bt} represents the rate constant for the back-electron transfer and k_p the rate constant of diffusive separation of the radical pair $^1(A^{\bullet(+Z_A-1)} \cdots Q^{\bullet(-Z_Q+1)})$. The lack of evidence for $A^{\bullet(+Z_A-1)}$ and $Q^{\bullet(-Z_Q+1)}$ in the transient spectra indicate that $k_{bt} \gg k_p$.

4. Conclusion

It was shown that the most likely mechanism of the quenching of acridine and its derivatives' fluorescence by sulfur-containing amino and carboxylic acids is the transfer of an electron from the sulfur atom of the quencher to the acridines' lowest excited singlet state. The singlet quenching is followed by fast back-electron transfer within the singlet radical ion pair $^1(A^{\bullet(+Z_A-1)} \cdots Q^{\bullet(-Z_Q+1)})$. The rate constant of the process was found to be dependent on the reactants' charge, reaching approximately one-half of the diffusion-controlled limit for the systems lacking Coulombic interactions. On the other hand, the systems with opposite charges on quencher and excited species had quenching rate constants that were essentially diffusion controlled. These trends in the quenching rate constants are rationalized in a semi-quantitative manner with Scheme 2 along with the assumption that the pre-exponential in the electron-transfer step does not vary with the charge on the quencher. There was a static component to the quenching as seen in fluorescence-intensity measurements that was ascribed to non-fluorescent ion pairs. The interionic distances computed from the experimental K_S values and the Fuoss equation are consistent with the ion pairs of the $Z_A Z_Q = -1$ and -2 cases being solvent-separated ion pairs while those of the $Z_A Z_Q = -3$ case are contact ion pairs.

Acknowledgements

References

[1] G.L. Hug, B. Marciniak, K. Bobrowski, J. Photochem. Photobiol. A 95 (1996) 81.
[2] M. Vogt, Free Radical Biol. Med. 18 (1995) 93.
[3] L.M. Sayre, M.G. Zagorski, W.K. Surewicz, G.A. Krafft, G. Perry, Chem. Res. Toxicol. 10 (1997) 518.
[4] D.A. Butterfield, Chem. Res. Toxicol. 10 (1997) 495.
[5] K. Sasaki, T. Hiroshima, S. Kususmoto, K. Nishi, Chem. Pharm. Bull. 37 (1989) 2160.
[6] D. Cipolla, S.J. Shire, in: J.J. Villafranca (Ed.), Techniques in Protein Chemistry, Vol. II, Academic Press, New York, 1991, pp. 543–555.
[7] K. Bobrowski, B. Marciniak, G.L. Hug, J. Photochem. Photobiol. A 81 (1994) 159.
[8] K. Bobrowski, J. Rozwadowski, J. Phys. Chem. 98 (1994) 4854.
[9] K. Bobrowski, B. Marciniak, G.L. Hug, J. Am. Chem. Soc. 114 (1992) 10279.
[10] K. Bobrowski, B. Marciniak, G.L. Hug, H. Kozubek, J. Phys. Chem. 98 (1994) 537.
[11] M. Goez, J. Rozwadowski, B. Marciniak, J. Am. Chem. Soc. 118 (1996) 2882.
[12] B. Marciniak, J. Rozwadowski, J. Photochem. Photobiol. A 101 (1996) 163.
[13] B. Marciniak, G.L. Hug, J. Rozwadowski, K. Bobrowski, J. Am. Chem. Soc. 117 (1995) 127.
[14] P. Hapiot, I. Moiroux, I.M. Saveout, J. Am. Chem. Soc. 112 (1990) 1337.
[15] J. Karolczak, D. Komar, J. Kubicki, M. Szymanski, T. Wrozowa, A. Maciejewski, Bull. Pol. A. Sci. Chem. 47 (1999) 361.
[16] M.D. Thomas, G.L. Hug, Comput. Chem. (Oxford) 22 (1998) 491.
[17] E. Pines, D. Huppert, M. Gutman, W. Nachliel, M. Fishman, J. Phys. Chem. 90 (1986) 6366.
[18] I.W. Bunting, W.G. Meathrel, Can. J. Chem. 52 (1974) 981.
[19] R.M. Smith, A.E. Martel, Critical Stability Constants, Vols. 1 and 6, Plenum Press, New York, 1974 and 1989.
[20] M. Fujita, A. Ishida, S. Takamuku, S. Fukuzumi, J. Am. Chem. Soc. 118 (1996) 8566.
[21] I.R. Lakowicz, Principles of Fluorescence Spectroscopy, Plenum Press, New York, 1983, p. 266.
[22] R.M. Fuoss, J. Am. Chem. Soc. 80 (1958) 5059.
[23] R.G. Wilkins, Kinetics and Mechanism of Reactions of Transition Metal Complexes, 2nd Edition, VCH, Weinheim, 1991.
[24] H.S. Harned, B.B. Owen, The Physical Chemistry of Electrolytic Solutions, 3rd Edition, Reinhold, New York, 1958.
[25] C.J.F. Böttcher, Theory of Electric Polarization, Vol. 1, 2nd Edition, Elsevier, Amsterdam, 1973.
[26] S.A. Rice, Comprehensive Chemical Kinetics, Vol. 25, Diffusion Limited Reactions, Elsevier, New York, 1985.
[27] D. Rehm, A. Weller, Isr. J. Chem. 8 (1970) 259.
[28] B. Marciniak, K. Bobrowski, G.L. Hug, J. Phys. Chem. 97 (1993) 11937.
[29] K.K. Chatterjee, S. Chatterjee, Z. Physik. Chem. Neue Folge 94 (1975) 107.
[30] R.E. Weston Jr., H.A. Schwarz, Chemical Kinetics, Prentice-Hall, Englewood Cliffs, NJ, 1972.
[31] G.G. Hammes, Principles of Chemical Kinetics, Academic Press, New York, 1978.
[32] M. Eigen, Z. Phys. Chem. (Leipzig) 1 (1954) 176.
[33] I. Carmichael, G.L. Hug, J. Phys. Chem. Ref. Data 15 (1986) 1.
[34] J.K. Hurley, H. Linschitz, A. Treinin, J. Phys. Chem. 92 (1988) 5151.
[35] H. Hiratsuka, K. Sekiguchi, Y. Hatano, Y. Tanizaki, Chem. Phys. Lett. 55 (1978) 358.
[36] K.O. Hiller, B. Masloch, M. Göbl, K.D. Asmus, J. Am. Chem. Soc. 103 (1981) 2734.
[37] K. Bobrowski, G.L. Hug, B. Marciniak, B. Miller, C. Schöneich, J. Am. Chem. Soc. 119 (1997) 8000.
[38] K.-D. Asmus, Nukleonika 45 (2000) 3.
[39] K.-D. Asmus, M. Bonifacic, in: Z.B. Alfassi (Ed.), S-Centered Radicals, Wiley, New York, 1999.